The Astrophysical Journal, 685:863–874, 2008 October 1

THE RED SEQUENCE OF HIGH-REDSHIFT CLUSTERS: A COMPARISON WITH COSMOLOGICAL GALAXY FORMATION MODELS

N. Menci,[1] P. Rosati,[2] R. Gobat,[2] V. Strazzullo,[3] A. Rettura,[4] S. Mei,[5] and R. Demarco[4]

Received 2008 January 7; accepted 2008 June 8

ABSTRACT

We compare the results from a state-of-the-art semianalytic model of galaxy formation with spectrophotometric observations of distant galaxy clusters observed in the range $0.8 \leq z \leq 1.3$. We investigate the properties of their red sequence (RS) galaxies and compare them with those of the field at the same redshift. In our model we find that (1) a well-defined, narrow RS is obtained already by $z \approx 1.2$; this is found to be more populated than the field RS, analogously to what is observed and predicted at $z = 0$; (2) the predicted $U-V$ rest-frame colors and scatter of the cluster RS at $z = 1.2$ have average values of 1 and 0.15, respectively, with a cluster-to-cluster variance of $\approx$0.2 and $\approx$0.06, respectively. The scatter of the RS of cluster galaxies is $\approx$5 times smaller than the corresponding field value; (3) when the RS galaxies are considered, the mass growth histories of field and cluster galaxies at $z \approx 1.2$ are similar, with 90% of the stellar mass of RS galaxies at $z = 1.2$ already formed at cosmic times $t = 2.5$ Gyr, and 50% at $t = 1$ Gyr; and (4) the predicted distribution of stellar ages of RS galaxies at $z = 1.2$ peaks at 3.7 Gyr for both cluster and field populations; however, for the latter the distribution is significantly skewed toward lower ages. When compared with observations, the above findings show an overall consistency, although the average value $\Delta_{U-V} \approx 0.07$ of the observed cluster RS scatter at $z \approx 1.2$ is smaller than the corresponding model central value. We discuss the physical origin and the significance of the above results in the framework of cosmological galaxy formation.

Subject headings: galaxies: clusters: general — galaxies: evolution — galaxies: formation

1. INTRODUCTION

Environment-dependent properties of galaxies constitute a natural test ground for cosmological theories of galaxy formation. These envisage the properties of the galaxy populations to originate from the primordial density field dominated by dark matter (DM); the collapse and growth of small-scale perturbations (leading to galaxy progenitors) is thus modulated by the underlying large-scale density field whose overdense regions will collapse to form groups and clusters of galaxies.

Among the galaxy properties, the color distribution constitutes a major issue, as colors measure the ratio of the present star formation rate to the overall mass of formed stars in a given galaxy. Three fundamental observational results deal with the star formation history and the color distribution of field galaxies: (a) the global star formation decrease from $z = 1.5$ to the present by almost 2 dex (see, e.g., the compilation by Hopkins [2004] and references therein); (b) the downsizing (Cowie et al. 1996), i.e., a stronger ($\sim$3 dex) and earlier (starting at least at $z \approx 2$) decline of star formation in massive galaxies compared to a slower ($\approx$1 dex) decline of the star formation rate of the present blue/late-type galaxies from $z \sim 1.5$; correspondingly, an inverse correlation of the age of the stellar population with the galaxy stellar mass is observed; and (c) the bimodality (Strateva et al. 2001; Baldry et al. 2004; Bell et al. 2004), i.e., a marked segregation in color between the blue galaxy population (dominant at faint magnitudes and for low-mass galaxies) and the red population (dominant for bright, massive galaxies) populating the "red sequence" (RS).

In hierarchical clustering models, the first property naturally results from the high star formation rate at high redshifts $z \gtrsim 2$ sustained by the high cooling efficiency in the dense environments of galaxy progenitors and by effective starbursts; the decline at $z \lesssim 2$ follows from the exhaustion of the gas reservoir converted into stars at higher z. The interpretation of downsizing in hierarchical galaxy formation is also straightforward: bright, massive galaxies form from the coalescence of protogalaxies which collapsed in a biased, overdense region of the primordial density field; thus, such progenitors collapsed and began to form stars at earlier cosmic epochs, and their cold gas reservoir is exhausted earlier, thus yielding older (and hence redder) stellar populations in the final galaxy. The origin of the bimodality is more controversial; recent works (see discussion in Neistein et al. 2006; Dekel & Birnobim 2006; Menci et al. 2006) suggest that self-regulation of star formation (due to supernovae feedback) can be effective below a critical (DM) mass scale $M \approx 5 \times 10^{11}\ M_{\odot}$; the inclusion of feedback from active galactic nuclei (AGNs) then quenches further star formation in massive halos.

The above properties are strongly modulated by the galaxy environment. Not only has the morphology long been recognized to strongly depend on the environment (with the fraction of early-type galaxies increasing in groups and clusters of galaxies; Spitzer & Baade 1951), but also the fraction of galaxies belonging to the blue population has been recently recognized to decrease in dense environments (Baldry et al. 2004, 2006; Gerke et al. 2007; Cooper et al. 2006). The environmental dependence of the blue fraction f_b is stronger than the above-mentioned luminosity dependence observed in the field. This means that the environmental density enhances the probability for an early star formation followed by quenching even for low- or intermediate-mass galaxies.

The scenario emerging from the above observational framework is the following: galaxies flow from the blue population to the RS (corresponding to the decline of star formation at $z < 2$) at rates and cosmic epochs that depend very strongly on their mass and environment. Massive galaxies have converted most of their

[1] INAF–Osservatorio Astronomico di Roma, via di Frascati 33, I-00040 Monteporzio, Italy.
[2] European Southern Observatory, Karl-Schwarzschild-Strasse 2, D-85748 Garching, Germany.
[3] National Radio Astronomy Observatory, P.O. Box O, Socorro, NM 87801.
[4] Department of Physics and Astronomy, Johns Hopkins University, Baltimore, MD 21218.
[5] GEPI, Observatoire de Paris, Section de Meudon, 92195 Meudon Cedex, France.

gas into stars and moved to the RS very early at $z > 2$ in both cluster and field, since at high redshift their star formation was not effectively self-limited by feedback. On the other hand, lower mass galaxies $M < 10^{12}\ M_{\odot}$ move to the RS later in the field compared to clusters. The speedup of the transition to the RS of intermediate-/low-mass galaxies in dense environments (groups and clusters) can be contributed by a number of physical processes. (i) Biased galaxy formation: in principle, galaxies later included in groups and clusters form from clumps which collapsed in biased, overdense regions of the primordial field, hence characterized by an earlier star formation. However, the initial overdensity corresponding to the final group or cluster may be so tiny that such an effect might be too small. (ii) Starbursts resulting from galaxy merging and flyby (sometimes referred to as "harassment"): while merging is actually enhanced in groups compared to clusters (see Cavaliere et al. 1992), the minor—but more frequent—starbursts originated from galaxy grazing encounters may significantly accelerate the star formation at high redshift in groups and clusters, and hence anticipate the transition to the RS. Note, however, that this process is effective mainly for midsize galaxies which strike the best compromise between cross section and abundance. (iii) Strangulation: in small-mass galaxies the gas may be stripped off when they are included in the cluster (Larson et al. 1980); in most semianalytic models this is captured by dispersing their hot gas mass through the whole host halo (see, e.g., Balogh et al. 2000). Note that our model, similarly to canonical semianalytic approaches, does not deal with the ram pressure stripping of the dense, cold gas in satellite galaxies. (iv) AGN feedback: to some extent, such a mechanism must be at work, and there is a general agreement (Ciotti & Ostriker 1997; Silk & Rees 1998; Haehnelt et al. 1998; Fabian 1999) that it may contribute to suppress any residual star formation in massive galaxies; in models where the AGN phase is triggered by galaxy interactions, the AGN feedback depends on the environment, which modulates the encounter probability. The effectiveness of the AGN feedback in quenching the black hole growth and the subsequent star formation has been confirmed by recent aimed simulations of galaxy collisions triggering AGN activity (Di Matteo et al. 2005). We have investigated the role of such a process in a previous paper (Menci et al. 2006), showing that it can affect the color distribution of most massive galaxies by removing the residual fraction of such galaxies that otherwise would populate the blue branch of the color distribution.

The relative role of all these processes is still a matter of investigation. Their dependence on the mass scale of the host structure (group or galaxy cluster) would provide an important clue to disentangle their contribution to the observed environment-dependent properties of galaxies. Several recent papers (Cooper et al. 2006; Gerke et al. 2007) point out that the difference in the properties of the RS between field and overdense environments remains unchanged up to $z \approx 1$, but tends to vanish at redshifts $z \gtrsim 1.3$. Since these results are based on samples which probe the environments up to the group scale (rich clusters are not included), the epoch $1.2 \lesssim z \lesssim 1.5$ would represent a measure of the effectiveness of poor/medium environments in modulating the star formation of member galaxies; at such redshifts, the environment-induced decline of the star formation would become stronger than the average cosmological decline. Probing the transition to the RS of galaxies in richer, extreme environments at $1 \lesssim z \lesssim 1.5$ is then crucial.

In this context, recent *Hubble Space Telescope* Advanced Camera for Surveys (*HST* ACS) observations of a sample of clusters at $0.8 < z < 1.3$ have fueled much progress; e.g., Blakeslee et al. (2003, 2006) and Mei at al. (2006a, 2006b) have found a well-defined and extremely narrow RS with an intrinsic scatter of $\sim$0.05 mag (in the color $i_{775} - z_{850}$, as observed with *HST* ACS), much smaller than the corresponding field RS. This points toward the existence of a strong environment-dependent effect, which, for galaxies in extremely dense environments, has already been effective at $z \approx 1.5$, thus supporting the view that the denser the environment, the earlier the transition to the RS.

How do such results compare with hierarchical models? While such models essentially capture the transition of faint galaxies to the RS (at least in the redshift range $z \leq 0.8$; see De Lucia et al. 2007; for results of hydro/*N*-body simulations see Romeo et al. 2008), the tightness of the RS constitutes an impressive constraint for them, since in the hierarchical scenario the growth of DM halos constitutes—on average—a gradual process, driven by the merging of subclumps, the progressive cooling of gas at the center followed by a quiescent star formation. Since the tightness of the observed RS indicates a fast transition of the galaxies to the same region of the color distribution acting on very short timescales in the early epochs, this is particularly challenging for hierarchical models, which predict clusters of galaxies to be the last structures to virialize (typically at $z < 2$). On the other hand, in such models, high-redshift clusters also constitute the most biased environments for galaxies to form, hence enhancing the effectiveness of the processes (i)–(iv) described above in accelerating the transition to the RS. Thus, comparing the observed properties of the RS in high-z clusters with model predictions constitutes an extremely sensitive probe of hierarchical models and of the physical processes there included.

Here we compare the results of a state-of-the-art semianalytic model of galaxy formation with the properties of the RS of galaxy clusters at high redshift, the most extreme (biased) galaxy environments observed so far. We also emphasize that the observations used in this work are currently the most suited for such an analysis, as with ACS observations in the i and z bands one can achieve the photometric accuracy to reliably estimate color scatters out to $z \sim 1.3$.

The model we adopt is well suited for such an investigation, since it includes all the processes (i)–(iv) discussed above, which are thought to contribute to the environmental dependence of the star formation histories. In particular, it includes both the burst of star formation due to grazing encounters (important in the early building up of massive galaxies) and a description of the AGN evolution which has been extensively tested against observations in both the optical (Menci et al. 2003) and X-rays (Menci et al. 2004b). In previous papers (Menci et al. 2005, 2006) we have successfully compared the model with observations concerning the galaxy color distribution at low redshifts as a function of both luminosity and environment, and at high redshift we showed how the inclusion of AGN feedback allows us to suppress residual star formation in massive galaxies yielding the observed abundance of extremely red objects.

The paper is organized as follows: in §§ 2 and 3 we briefly recall the main properties of the semianalytic model we use, and the observational data set we compare with. In § 4.1 we show the model results concerning the color-magnitude relation at both low and high redshift in the cluster and in the field, and we briefly discuss how it compares with existing observations. In § 4.2 we focus on the properties of the RS in high-redshift clusters, and compare the model results concerning the scatter and the normalization of the RS with the ACS observations of distant clusters. We also provide predictions concerning the distribution of the scatter and the normalization of the RS among the cluster population, which could be verified with existing or future observations. In § 4.3 we also compare the mass assembly history

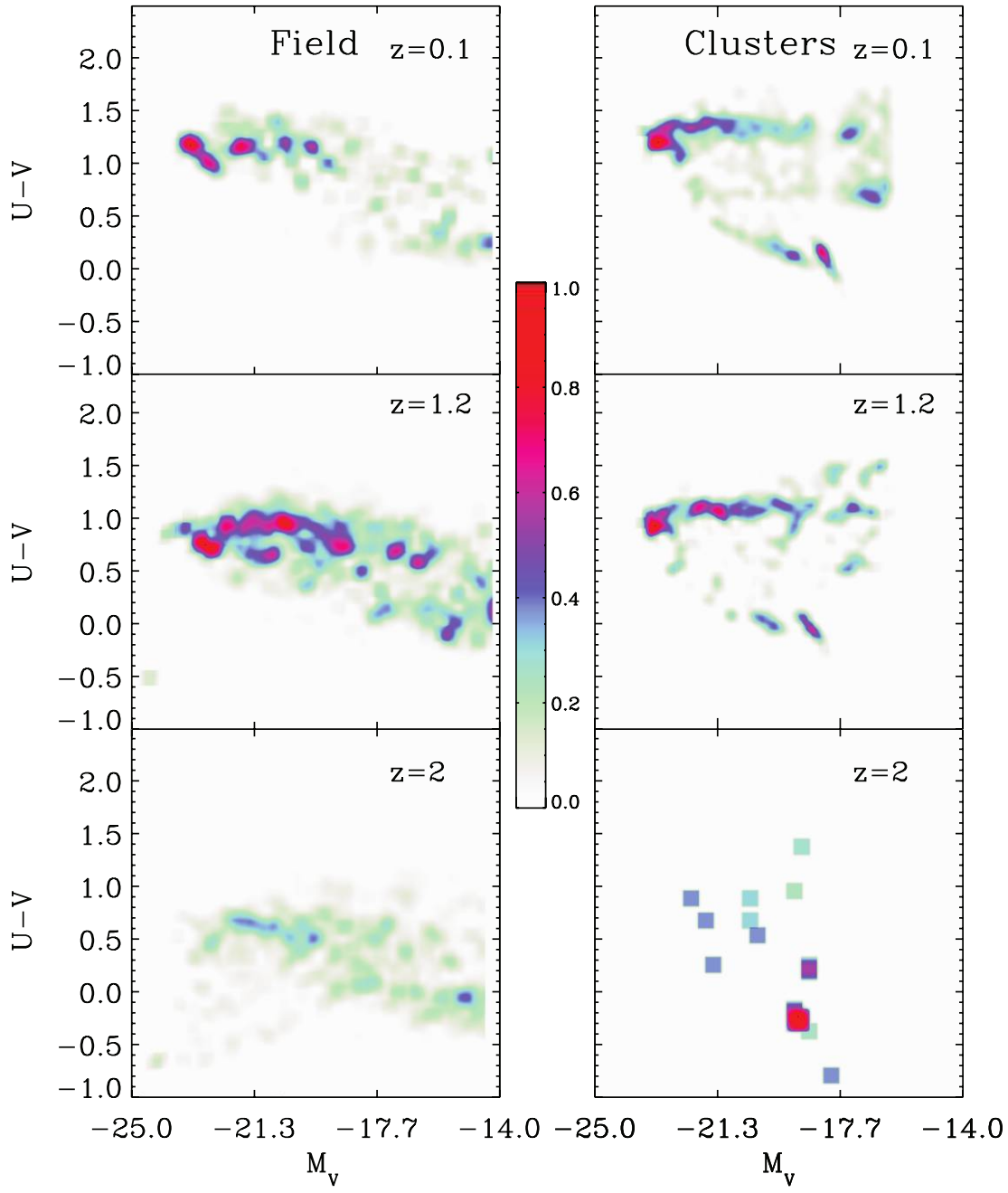

FIG. 1.—Color-magnitude ($U - V$ vs. V) relation computed from our model for all galaxies (*left panels*) and for galaxies hosted in rich groups or clusters (i.e., in halos with mass $M \geq 10^{14}\ M_{\odot}$; *right panels*) at $z = 0.1$, $z = 1.2$, and $z = 2$ (*from top to bottom*). The color code (*central color bar*) represents the number of galaxies in a given color-magnitude bin normalized to the abundance of galaxies at the considered magnitude.

and the age distribution of $z \approx 1.2$ galaxies in the field and in clusters resulting from the model with estimates derived from fitting observed galaxy colors and spectra with spectral synthesis models. In § 4.4 we interpret our results on the basis of the physical processes which determine the scatter of the RS in hierarchical models. In § 5 we draw our conclusions.

2. THE MODEL

Here we recall the key properties of the semianalytic model we adopt, referring to our previous papers for details. The DM halos of protogalaxies collapse from overdense regions of the primordial DM density field, taken to be a Gaussian random density field with a cold dark matter (CDM) power spectrum in a "concordance" cosmology with $\Omega_{\Lambda} = 0.7$, $\Omega_0 = 0.3$, baryonic density $\Omega_b = 0.04$, and Hubble constant (in units of 100 km s^{-1} Mpc^{-1}) $h = 0.7$. The normalization of the spectrum, in terms of the variance of the field smoothed over a region of $8\ h^{-1}$ Mpc, is taken to be $\sigma_8 = 0.9$. Since the rms value of the density field decreases with mass, progressively larger regions of the density field collapse with increasing time (eventually leading to the formation of groups and clusters of galaxies), and include the previously formed condensations. The corresponding merging rate of the DM halos is provided by the extended Press & Schechter formalism (see Bond et al. 1991; Lacey & Cole 1993) and implemented as described in detail in Menci et al. (2005, 2006). The clumps included into larger DM halos may survive as satellites, merge to form larger galaxies due to binary aggregations among satellites, or coalesce into the central dominant galaxy due to dynamical

friction. These processes take place over timescales which increase over cosmic times, so the number of satellite galaxies increases as the DM host halos grow from groups to clusters. All of the above processes are implemented using the usual prescriptions of semianalytic models as described in Menci et al. (2005, 2006).

We adopt the treatment of the baryonic processes described in our previous papers (Menci et al. 2005) with the same choice of free parameters. These include the cooling at the center of galaxies, the settling of the cooled gas with mass m_c into a rotationally supported disk with radius r_d and circular velocity v_d, the gradual (quiescent) conversion of such gas into stars at a rate $\dot{m}_*$, and the stellar feedback, which results in redistributing part of the cooled gas to the hot gas phase (with mass m_h) at the virial temperature of the halo. An additional channel for star formation implemented in the model is provided by interaction-driven starbursts, triggered not only by merging events but also by flyby events. Such a star formation mode provides an important contribution to the early formation of stars in massive galaxies, as described in detail in Menci et al. (2004a, 2005).

The model also includes a treatment of the growth of supermassive black holes at the center of galaxies by interaction-triggered inflow of cold gas, following the physical model in Cavaliere & Vittorini (2000). The accretion episodes, corresponding to the active AGN phases, also trigger the AGN feedback onto the surrounding cold gas, whose physical treatment is derived from Lapi et al. (2005). A detailed description and testing of such a section of the model is presented in Menci et al. (2006).

Thus, all processes which are candidates for enhancing the early star formation in galaxies in dense environments (and for the subsequent quenching of star formation) are included in the model. The distribution of gas mass, disk sizes, stellar masses, and luminosities have been checked against observations in previous papers, as well as the growth of AGNs and the corresponding redshift-dependent luminosity functions in both the optical and X-rays.

3. THE DATA SET

We compare our model mainly with the results from the *HST* ACS Intermediate Redshift Cluster Survey, which consisted of multicolor observations of eight clusters with redshifts in the interval $0.8 \leq z \leq 1.3$. We focus on the observations of the RS of these clusters, as described in Blakeslee et al. (2003, 2006), Homeier et al. (2006), and Mei et al. (2006a, 2006b, 2008). We also use the analysis by Gobat et al. (2008) and Rettura et al. (2008) of the 10-band spectral energy distributions (SEDs) and spectra of the early-type galaxies in RDCS 1252, the cluster at $z = 1.24$ with the best available multiwavelength data set in the cluster sample of early-type galaxies (Demarco et al. 2007). When comparing with the field data we use the spectroscopic sample of early-type galaxies in the GOODS-S field from the Vanzella et al. (2008) study, with masses determined from the multiwavelength data set offered by the GOODS survey (Rettura et al. 2006).

4. RESULTS

4.1. *The Color-Magnitude Diagram of Cluster versus Field Galaxies*

The color-magnitude diagram ($U - V$ color vs. absolute V magnitudes in the Vega system) obtained from the model is shown in Figure 1 for both field (*left*) and cluster galaxies (*right*) in three redshift bins. The color code corresponds to the density of galaxies in a given color and luminosity bin divided by the density of galaxies in the considered luminosity bin. Note that the cluster color-magnitude diagram does not correspond to galaxies residing in a single cluster, but it refers to all galaxies residing in host DM halos more massive than $10^{14}\ M_\odot$.

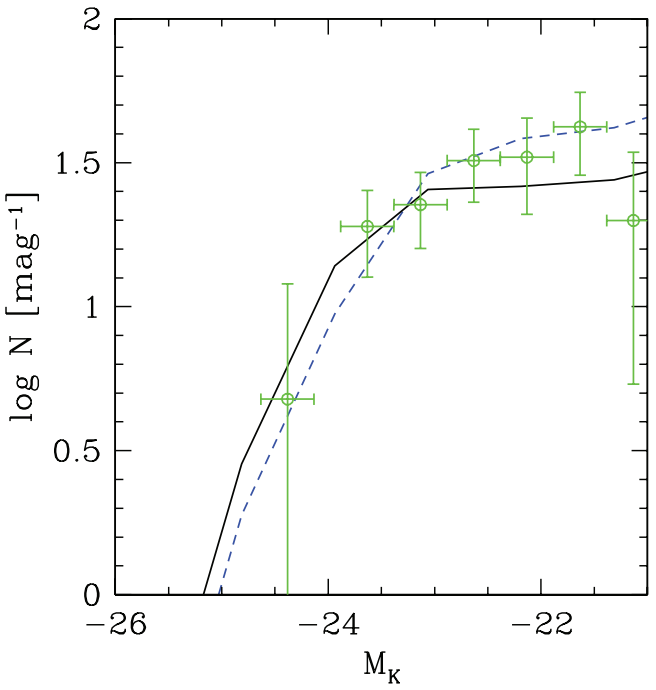

FIG. 2.—*K*-band luminosity function at $z = 1.2$ from our model (*solid line*) compared with data obtained from near-infrared images of three distant X-ray clusters with an average redshift $z \approx 1.2$ (Strazzullo et al. 2006). We have checked the normalization of the model luminosity functions by comparing the abundance of bright model galaxies with the observations at both low and high redshifts (see text). For comparison, we also show the luminosity function of model field galaxies at the same redshift $z = 1.2$ (*dashed line*). For graphical reasons, its actual normalization (predicted by the model), has been rescaled to match the value of the cluster luminosity function at the characteristic luminosity M_{K*}.

Before discussing in detail the features of the color-magnitude relation, we first check that the magnitude distribution of galaxies predicted by the model is consistent with the observations. While at low redshift the abundance of red galaxies in dense environments (as well as in the field) has been checked against observations in Menci et al. (2005), here we explore it at the highest available redshift in Figure 2, where we perform a detailed comparison of the $z = 1.2$ *K*-band luminosity function from our model with the available observations of high-redshift clusters (Strazzullo et al. 2006). The model field luminosity function is also shown as a dashed line; for graphical reasons, its actual normalization (predicted by the model) has been rescaled to match the cluster luminosity function at the characteristic luminosity M_{K*}.

For the model cluster luminosity function shown in Figure 2, we have checked that its normalization is consistent with the observed abundance of bright galaxies, at both low and high redshifts. Indeed, the model predicts a cosmic density (per Mpc^3) of bright ($M_K < -20$) galaxies, located in clusters with mass $M > 10^{14.5}\ M_\odot$ at $z = 1.2$ (corresponding to the average X-ray luminosity of the cluster sample adopted in Strazzullo et al. [2006] using the same conversion adopted by such authors), which is 3% of the overall (field) density of model galaxies with the same brightness at such redshift. This ratio between the cluster and the field density predicted by the model is in good agreement with the observational value estimated by Strazzullo et al. (2006) at the same redshift (4%–5 % of bright galaxies are found in clusters). Thus, a small uncertainty (a logarithmic factor

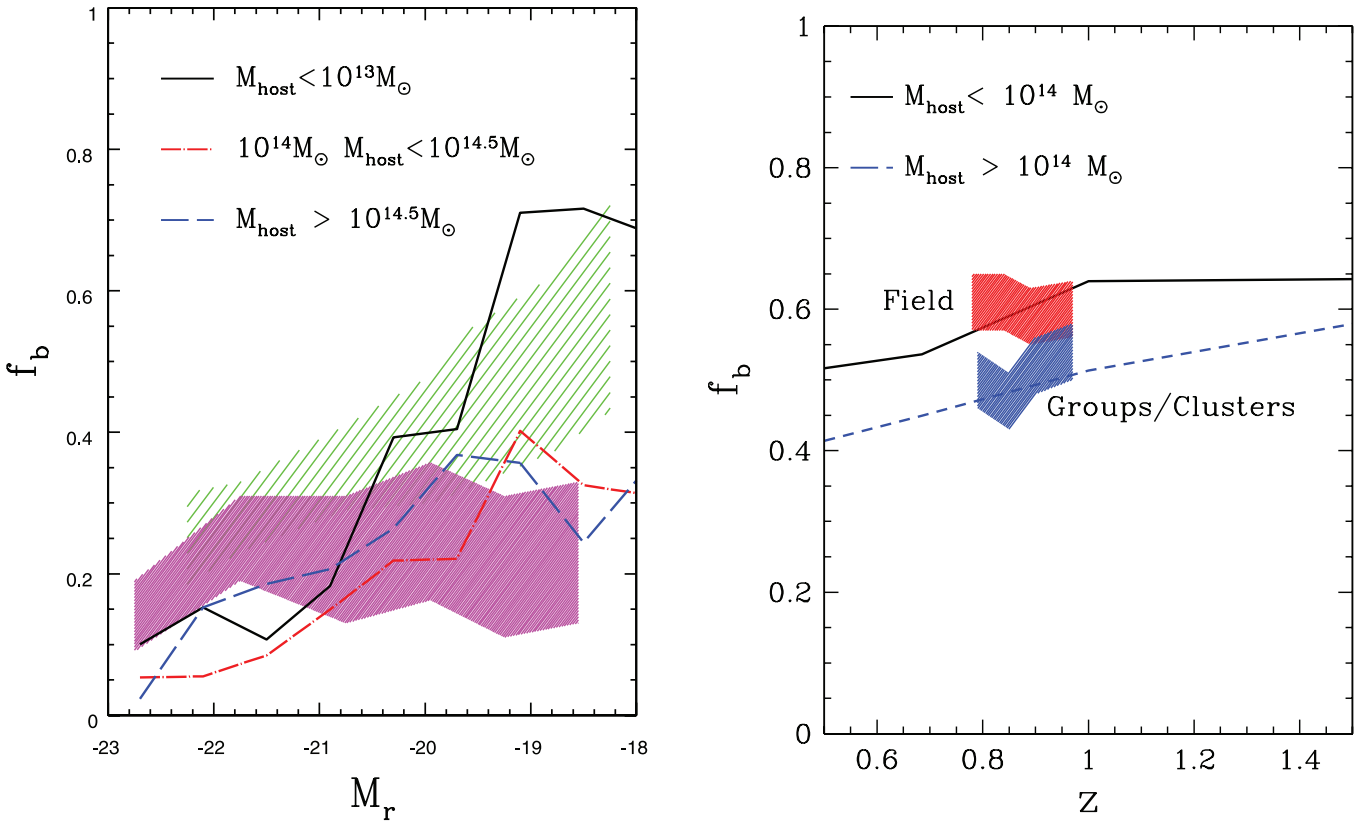

FIG. 3.—Model blue fraction (*lines*) compared with available data for different environments as a function of the *r*-band absolute magnitude in the local universe (*left*) and of redshift (*right*). To perform a proper comparison, the blue fraction f_b in the two panels has been computed adopting the same magnitude cut adopted in the papers we compare with, as detailed below. *Left*: The fraction of $z = 0.1$ galaxies bluer than $(g - r)_{\rm cut} = 0.7 - 0.032(M_r + 16.5)$ (where the SDSS absolute magnitudes *K*-corrected to $z = 0.1$ are adopted as in Weinmann et al. [2006]), is shown as a function of M_r for model galaxies hosted in halos with different mass, as indicated by the different line types. For comparison, we have also included the observational results obtained from the SDSS group catalog described in detail in Weinmann et al. (2006): the upper shaded area corresponds to galaxies in host halos with mass $10^{12.5}\ M_\odot \le M \le 10^{13}\ M_\odot$, while the lower one corresponds to galaxies in clusters with $10^{14}\ M_\odot \le M \le 10^{14.5}\ M_\odot$. *Right*: To compare with the observations from the DEEP2 survey (Gerke et al. 2007), the fraction of galaxies bluer than $U - B = -0.032(M_B - 5\log h + 21.62) + 1.2$ and magnitudes brighter than $M_B - 5\log h = -20.7 - 1.37(1 - z)$ is shown as a function of redshift for model field galaxies (*solid line*) and for model galaxies in groups/clusters (with halo mass $M \ge 10^{14}\ M_\odot$; *dashed line*). The shaded regions correspond to the results from the sample I in Gerke et al. (2007) for field galaxies (*upper region*) and group galaxies (*lower region*).

of 0.15) in the relative normalization of the observed and the model luminosity function in Figure 2 is present. It is interesting to note that the broad agreement between the model and the observations concerning the fraction of bright galaxies located in massive clusters persists down to redshift zero, where the observations yield values of 6%–7% compared to a predicted value of ≈10%. Finally, we also show in Figure 2 the model luminosity function predicted for the field at the same redshift. Note that the model luminosity function shows little dependence on the environment (in agreement with observations by Strazzullo et al. [2006]), although the model yields a somewhat larger abundance of massive galaxies in clusters compared to the field.

Having checked the abundance of galaxies as a function of their magnitude against observations, we now examine in detail the properties of the color-magnitude distribution shown in Figure 1. First, we note that the overall trend of brighter galaxies to be redder than fainter ones is effectively modulated by the environment, so that the fraction of faint galaxies with red colors is larger in clusters than in the field up to $z \approx 1.5$–2. This reflects the shift of color distribution of faint galaxies toward red colors in dense environments already shown for local galaxies (Menci et al. 2005), and constitutes a first-order consistency check with local observations (Baldry et al. 2004) and with the observed trend in groups up to $z \approx 1.3$ (Gerke et al. 2007).

Here such a check is extended to the richest environments at higher redshifts and to a wider magnitude range in Figure 3. In particular, the local fraction of blue galaxies (f_b; see caption for the definition) is shown as a function of absolute magnitude for small ($M/M_\odot \le 10^{13}$) and large ($M/M_\odot \ge 10^{14}$) host halo masses, and compared with the Sloan Digital Sky Survey (SDSS) data group catalog (Weinmann et. 2006) in Figure 3 (*left*). The decrease of f_b with increasing density of the environment, especially marked for faint galaxy magnitudes, is not unexpected in hierarchical theories [see point (i) in § 1]. It traces back to the properties of the primordial density field: galaxies in groups/clusters are formed from the collapse of clumps within biased, high-density regions of the primordial field, where the enhanced density allowed for an earlier (and higher) star formation activity. The gas conversion into stars is thus anticipated, and the rate of galaxy transition from the blue cloud to the RS is accelerated, leading to a higher fraction of red galaxies at $z \lesssim 2$.

Second, we note from Figure 1 that at bright magnitudes, the color distribution is *entirely* dominated by red objects (see also Fig. 3, *left*). The origin of such an effect has been discussed in several papers (see, e.g., Bower et al. 2006; Menci et al. 2005). On the one hand, the downsizing (i.e., the color/age-luminosity correlation) is a natural outcome of hierarchical models, since star formation within the progenitors of massive galaxies was enhanced at high redshift due to the biasing effect discussed above. On the

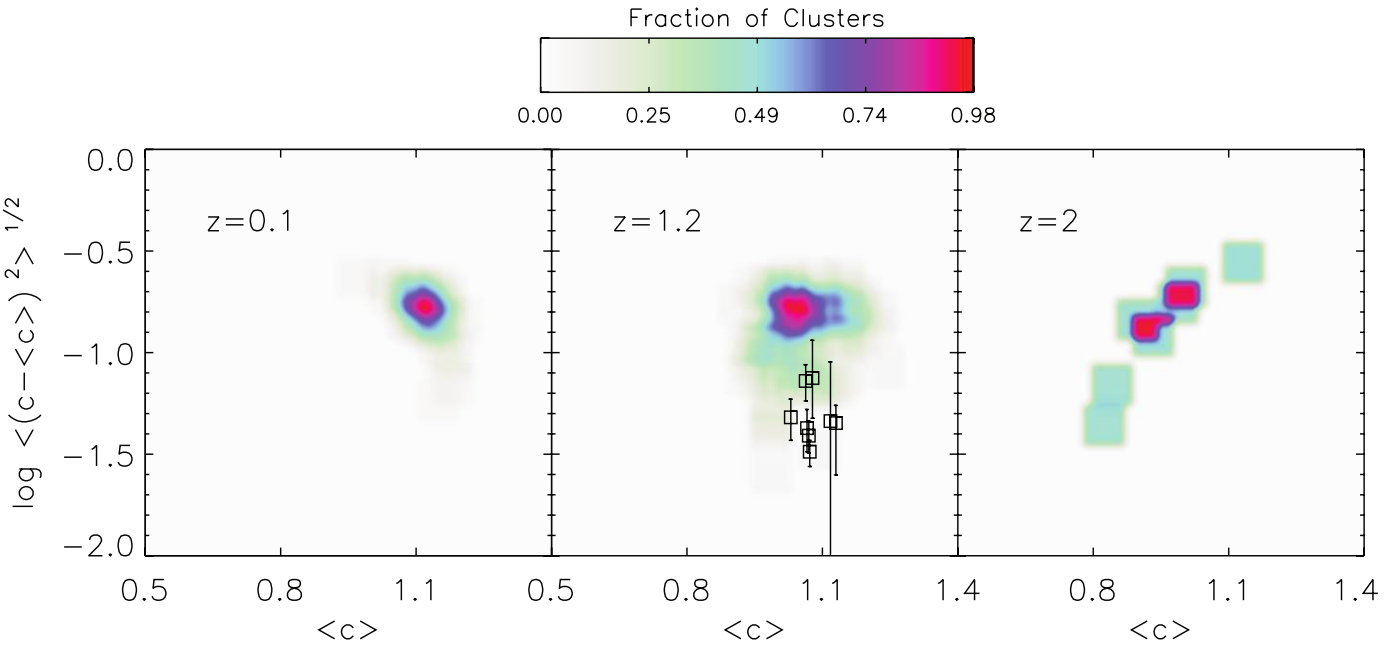

FIG. 4.—Normalization and scatter of the RS among the modeled cluster population. The RS is defined as the region of the color-magnitude plane (Fig. 1) with $c \equiv U - V > 0.8$, and for this we compute the average color $\langle c \rangle$ and the dispersion $\langle (c - \langle c \rangle)^2 \rangle^{1/2}$ around the average. The applied color cut is consistent with the minimum in the color distribution, which separates the two peaks corresponding to the blue and red populations (see Fig. 1 and the color distribution in the AB magnitude system computed in Menci et al. [2005, 2006]). The color code in the figure corresponds to the fraction of model clusters with given RS scatter $\langle c \rangle$ and normalization $\langle (c - \langle c \rangle)^2 \rangle^{1/2}$. For comparison, we also show in the same plane the points that correspond to eight observed clusters in the redshift range $0.8 \leq z \leq 1.3$ from the papers cited in § 3.

other hand, the probability of grazing encounters triggering bursts of star formation [see point (ii) in § 1] is larger for massive galaxies (with larger cross section) at high redshift (where the densities are larger), thus contributing to the early conversion of gas into stars for massive group/cluster member galaxies. However, a substantial fraction (≈40%; see Menci et al. 2006) of blue, massive galaxies would persist without the inclusion of AGN feedback in the model. This effectively suppresses residual star formation in massive halos, thus determining the extremely low fraction of massive (bright) blue galaxies.

At higher redshift, the overall redshift dependence of the blue fraction for bright galaxies (see caption) in clusters and in the field is shown in Figure 3 (*right*). This shows that the blue fraction predicted in clusters is larger than in the field up to $z = 1.5$. This is not unexpected, since high-redshift clusters (although rare) constitute the most biased environment for galaxy formation at high redshift, where the acceleration of star formation at $z > 2$ due to the processes mentioned above is maximally effective. Our results concerning the transition of faint galaxies to the RS in clusters of galaxies are consistent with the findings of other semianalytic models (De Lucia et al. 2007), and extend to higher redshifts $z \approx 1.2$; our results are also consistent with existing hydrodynamical *N*-body simulations (Romeo et al. 2008).

Thus, the rate of transition of galaxies from the blue cloud to the RS is reasonably well described in the hierarchical clustering model, so that it can be reliably used to gain insight on the properties of the RS galaxies, on which we focus next.

4.2. *The Properties of the RS in Clusters of Galaxies*

The most striking feature of the color-magnitude diagram resulting from the model (Fig. 1) is the extremely reduced scatter of the RS in clusters compared to the field, not only at low redshift but even at $z > 1$. When the cluster-to-cluster distribution of the RS scatter and normalization are examined (see Fig. 4), we find that all clusters are predicted to have a RS color scatter $\langle (c - \langle c \rangle)^2 \rangle^{1/2}$ (where $c \equiv U - V$) lower than 0.2 mag, and that the region enclosing 75% of the model clusters includes values of the RS scatter $\langle (c - \langle c \rangle)^2 \rangle^{1/2}$ smaller than 0.1 mag. Such very narrow RS is predicted for all clusters up to $z = 2$. The high-z values of the scatter and normalization of the RS resulting from the model are compared in detail with those observed in the distant cluster sample (§ 3) in Figure 5.

Note that an exact comparison between observed and model RS scatter constitutes a delicate point, since the observational morphological selection and the outlier rejection criteria adopted in the data analysis may affect the comparison with the model, which includes exact cluster members with any morphological types. In the original analysis of observed cluster data performed in the papers cited in § 3, only early-type galaxies were included: the corresponding observational results are represented by the square data points (with the errors given by the smaller error bars) in Figure 5. For the sake of a more accurate comparison to the model, we have recalculated the RS scatters for the same observed sample using a procedure as close as possible to the one adopted for model galaxies. In particular: (1) we included all RS (rest-frame $U - V > 0.8$) galaxies, irrespective of their morphological type, as in the model; (2) recomputed isophotal colors as from Sextractor (Bertin & Arnouts 1996); and (3) performed a 3 σ cut selection and made use of the available spectroscopic redshifts where available to reject outliers. The observational RS scatters are computed as $\langle (c - \langle c \rangle)^2 \rangle^{1/2}$, as done for model galaxies. The results from this new analysis of cluster data are to be considered as upper limits to the actual RS scatters due to the contamination from outliers. The larger possible values for the observational RS scatters (including the uncertainties) resulting from our new analysis are shown as downward-pointing arrows in Figure 5. The exact observational RS scatters to be compared with the model would lie between these upper limits and the square data points, and would have to include spectroscopically confirmed members for all morphological types (data that we do not have at present).

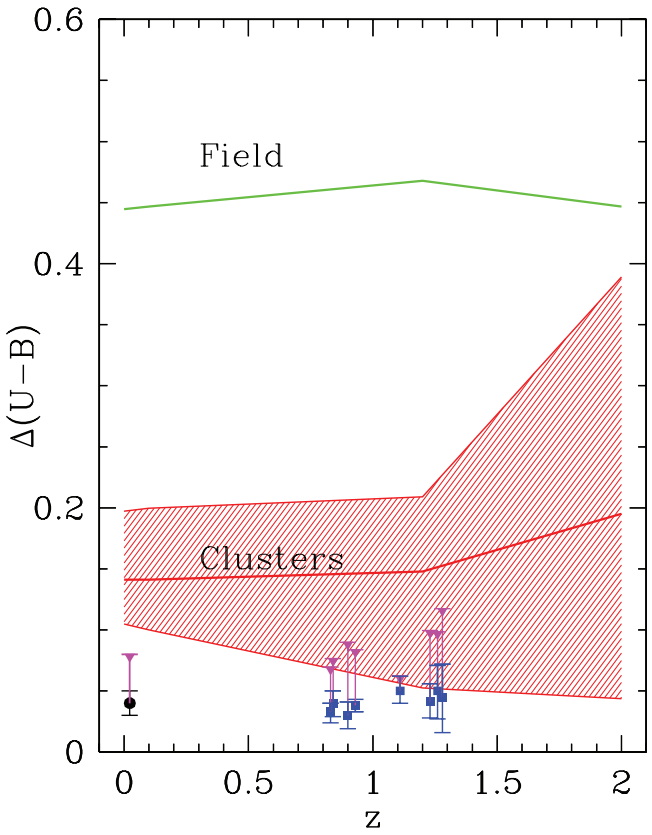

FIG. 5.— Comparison between predicted and observed scatters of the RS in high-redshift clusters. The lower shaded area represents the region enclosing 75% of the clusters in our Monte Carlo computation; the observational data points (*squares*) are taken from Blakeslee et al. (2003, 2006), Homeier et al. (2006), and Mei et al. (2006a, 2006b). The low-redshift point corresponds to the RS $U - V$ scatter of the Coma cluster measured by Bower et al. (1998). The downward-pointing arrows above all data points indicate the upper limits on the observed RS scatter obtained from our new data analysis, which includes galaxies of any morphological type (see text). For comparison, we also show our estimate of the scatter of the RS for model field galaxies (*upper solid line*).

Although appreciably smaller than the corresponding field value, the model RS scatter $\langle (c - \langle c \rangle)^2 \rangle^{1/2}$ for clusters is generally slightly larger than the observed values at high redshifts, which lie in the lower envelope of the region enclosing 75% of the model clusters (the light blue region in Fig. 4, and the shaded lower area in Fig. 5). It is also interesting to note that the model predicts a RS of high-z clusters with no universal average color, but rather with cluster-to-cluster variance of about 0.2 mag in $\langle c \rangle$. This is expected, since at high redshift clusters are still forming, so that the distribution of average colors reflects the different formation paths of these structures which are just emerging from the density field. Such a prediction is in agreement with the *HST* ACS observations, as is shown in the center panel of Figure 4, where the points corresponding to observed clusters show RS colors differing by $\approx$0.2 mag. Note that the average value of the RS scatter in the model decreases with redshift from $z = 2$ to $z = 0$ (see the red solid line in Fig. 5). The dispersion around such an average scatter decreases with redshift (see shaded area in Figs. 5 and 4), since different merging histories of subclusters formed at high redshift with different masses are included into a unique rich cluster at low redshift.

Thus, the model seems to capture the basic processes responsible for the narrow scatter of the RS of clusters, although the observations still lie on the envelope of the distribution of simulated clusters, which have a mean scatter at least twice as large as the observed one. The origin of this general behavior must be traced back to the fact that RS galaxies in high-redshift clusters are those formed in the most biased environment existing at those redshifts, so two possibilities arise to explain such an effect. (1) The peak of the *star formation history* of RS galaxies in clusters is shifted to earlier cosmic times compared to RS galaxies in the field, thus compressing the star formation activity of the progenitors of RS cluster galaxies in a narrow time range. In this case, the dense environment would not only accelerate the transition from the blue cloud to the RS (thus depressing f_b in clusters), but also affect the ages of galaxies which have already moved to the RS. (2) The effect is due to an intrinsic lower scatter in the *mass assembly history* of RS galaxies in clusters with respect to the field. This means that the number of possible paths along the merger trees leading to RS galaxies is smaller for galaxies in clusters compared to the field. We investigate both possibilities below.

4.3. *The Mass Growth History and the Age Distribution of Cluster versus Field Galaxies*

In Figure 6 we show the model predictions for the mass growth histories of field and cluster galaxies for galaxies belonging to the RS (i.e., with color $U - V \geq 0.8$) with stellar masses in the range $5 \times 10^{10} \leq M_*/M_\odot \leq 5 \times 10^{11}$. The color code refers to the fraction of galaxies which (at the given cosmic time shown in the x-axis) has attained the fraction of final stellar mass shown in the y-axis. The observational results (*square data points with error bars*) are from Gobat et al. (2008), who used two samples of spectroscopic early-type galaxies in the same stellar mass range drawn from the GOODS field (Vanzella et al. 2008) and the massive cluster RDCS 1252 at $z = 1.24$ (Demarco et al. 2007), and derived the star formation histories by fitting both their spectral energy distributions and spectra with a large grid of Bruzual & Charlot (2003) models.

Inspection of Figure 6 shows that in the hierarchical model the *average* stellar mass growth of cluster galaxies does not differ substantially from the field *when only RS galaxies are considered*; it is only the *fraction* of galaxies belonging to the RS which strongly depend on the environment, as discussed in the previous section. Comparison with the data shows a global consistency between expected and observed growth histories, although observations suggest slightly earlier stellar mass formation in cluster galaxies compared to the model. We should stress, however, that while the model mass growth histories are computed self-consistently from the star formation histories resulting from Monte Carlo merging tree simulations, the data points have been obtained by fitting star formation histories based on Bruzual-Charlot models with adjustable parameters affected by some degeneracies.

Figure 6 also shows that a major difference between the model cluster and field galaxies is in the *scatter* of the mass growth histories, which is much smaller for cluster galaxies compared to the field. For example, while there is a substantial fraction of field galaxies which have assembled only 60% of their stellar mass after 2 Gyr, almost all cluster galaxies have assembled more than 75% of their stellar mass at the same cosmic time. Thus, the small scatter observed in the cluster RS seems to be originated from a smaller dispersion in the mass growth histories of galaxies rather than from an earlier overall stellar mass growth. This is confirmed by the analysis of the distribution of stellar ages shown in Figure 7. We define star formation weighted ages as

$$\tau(t) = \frac{\int_0^t dt'(t - t')\dot{m}_*(t')}{\int_0^t dt'\dot{m}_*(t')}, \quad (1)$$

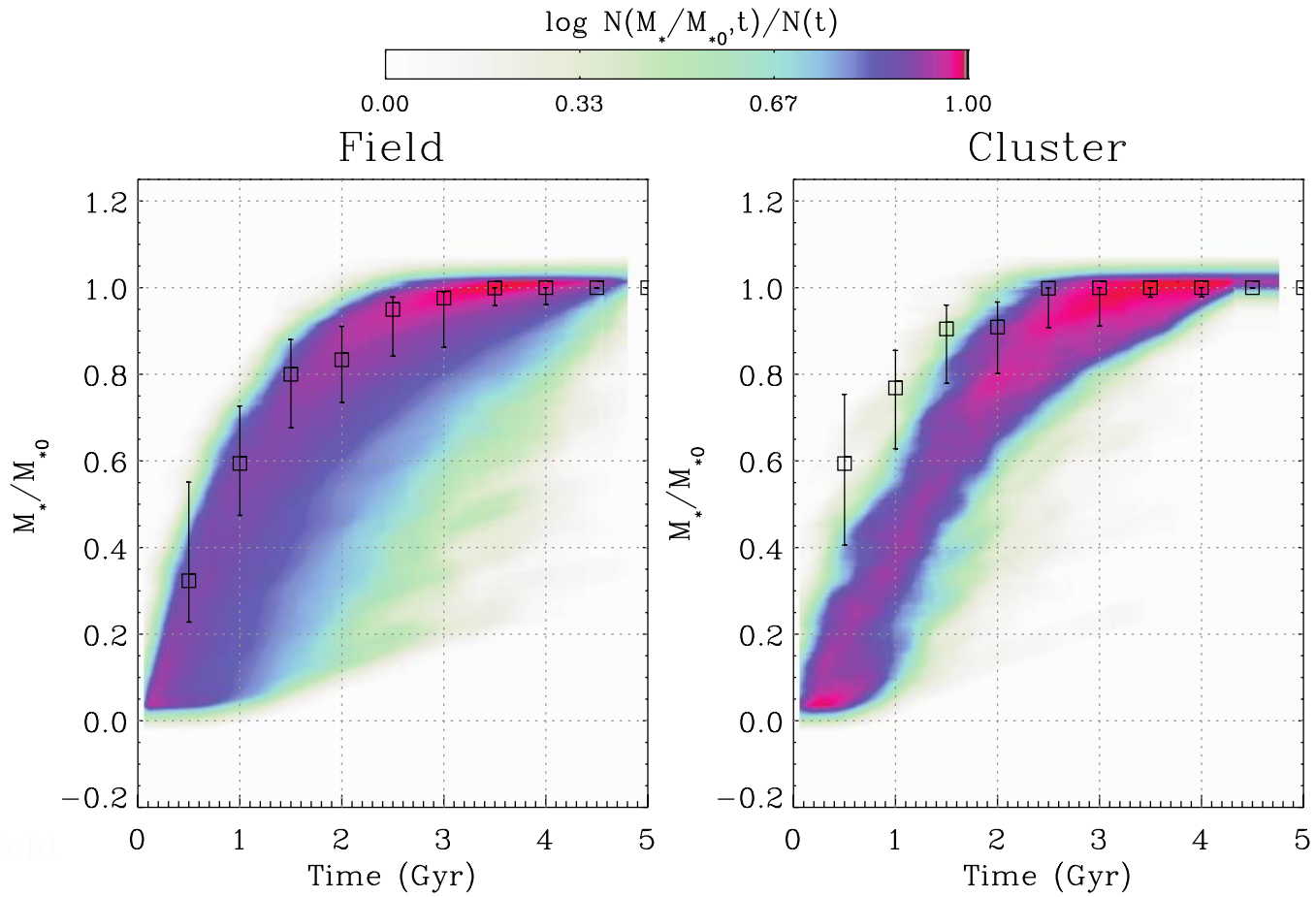

FIG. 6.— Stellar mass growth history of galaxies at $z = 1.2$ with stellar masses in the range $5 \times 10^{10} \leq M_*/M_\odot \leq 5 \times 10^{11}$. The mass fraction M_*/M_{*0} (y-axis) formed at the cosmic time t (x-axis) is computed as the stellar mass contained in all progenitors of each considered galaxy at $z = 1.2$ divided by its final (at $z = 1.2$) stellar mass. The color code represents the number of galaxies with given M_*/M_{*0} at a cosmic time t normalized to the total number of galaxies at that time. The data points, from Gobat et al. (2008), are derived from spectrophotometric observations of early-type galaxies in the field and in a rich cluster at $z = 1.24$, with stellar masses in the same mass range.

where t is the cosmic time at which we compute the average age of the stellar populations, and $t - t'$ is the age of the populations formed at time t' at a rate $\dot{m}_*(t')$. This definition has the advantage of taking into account the effective fraction of stellar mass contributed by each stellar population included in the average. Thus, the ages of the stellar populations contributing only a negligible fraction of the final stellar mass do not affect appreciably the average age defined by equation (1).

The predicted distribution of such quantity among the RS galaxy population in field and clusters at $z = 1.2$ is shown in the figure for the whole range of galaxy masses (*bottom panel*) and for the stellar mass range $5 \times 10^{10} \leq M_*/M_\odot \leq 5 \times 10^{11}$ (*top panel*) used in Figure 7.

The bottom panels of Figure 7 show an evident downsizing in both the field and cluster distributions, in the form of increasing average stellar ages with increasing galaxy stellar mass. This is consistent with a parallel analysis of observations by Rettura et al. (2008) of the same field and cluster samples used by Gobat et al. (2008). The top panels also show a good agreement between model predictions for star formation weighted ages and those derived from the spectrophotometric data (Gobat et al. 2008). In particular, the peak values of the stellar ages in the field and in clusters do not differ substantially in the considered mass range (a confirmation of our results on the stellar mass growth). However, while the cluster galaxies have a distribution neatly peaked around the median value, the age distribution of field galaxies shows a larger scatter with a tail toward shorter ages; the fraction of galaxies with ages shorter than 2 Gyr is negligible in clusters but is around 0.25 in the field.

Thus, both observational and model results concur in indicating that the smaller scatter of the RS in rich clusters compared to the field at high z cannot be accounted for by the difference in stellar mass assembly between field and cluster RS galaxies; however, such a (tiny) difference (not reproduced by the model; see right panel in Fig. 6) may be responsible for the residual discrepancy (a factor of $\approx$1.5) between the observed and the model RS, shown in Figures 4 and 5. We will come back to this point in § 5.

4.4. *Discussion: The Origin of Reduced Scatter in the Stellar Mass Assembly of Cluster Galaxies*

To understand the origin of the reduced scatter of the ages, color, and mass growth histories of cluster galaxies compared to the field, we show in Figure 8 (*top panels*) the model results concerning the ratio between the star formation contributed by minor progenitors (i.e., all progenitor DM halos except the main one) to that contributed by the main progenitor, as a function of cosmic time and final (at $z = 1.2$) galaxy stellar mass. Clearly, minor progenitors of cluster galaxies have contributed significantly to the stellar mass growth only at very early epochs, when they had all comparable masses. At times $t \gtrsim 1$ Gyr the contribution from minor progenitors is negligible, and the bulk of the stellar mass is formed in the main progenitors. Conversely, for field galaxies the

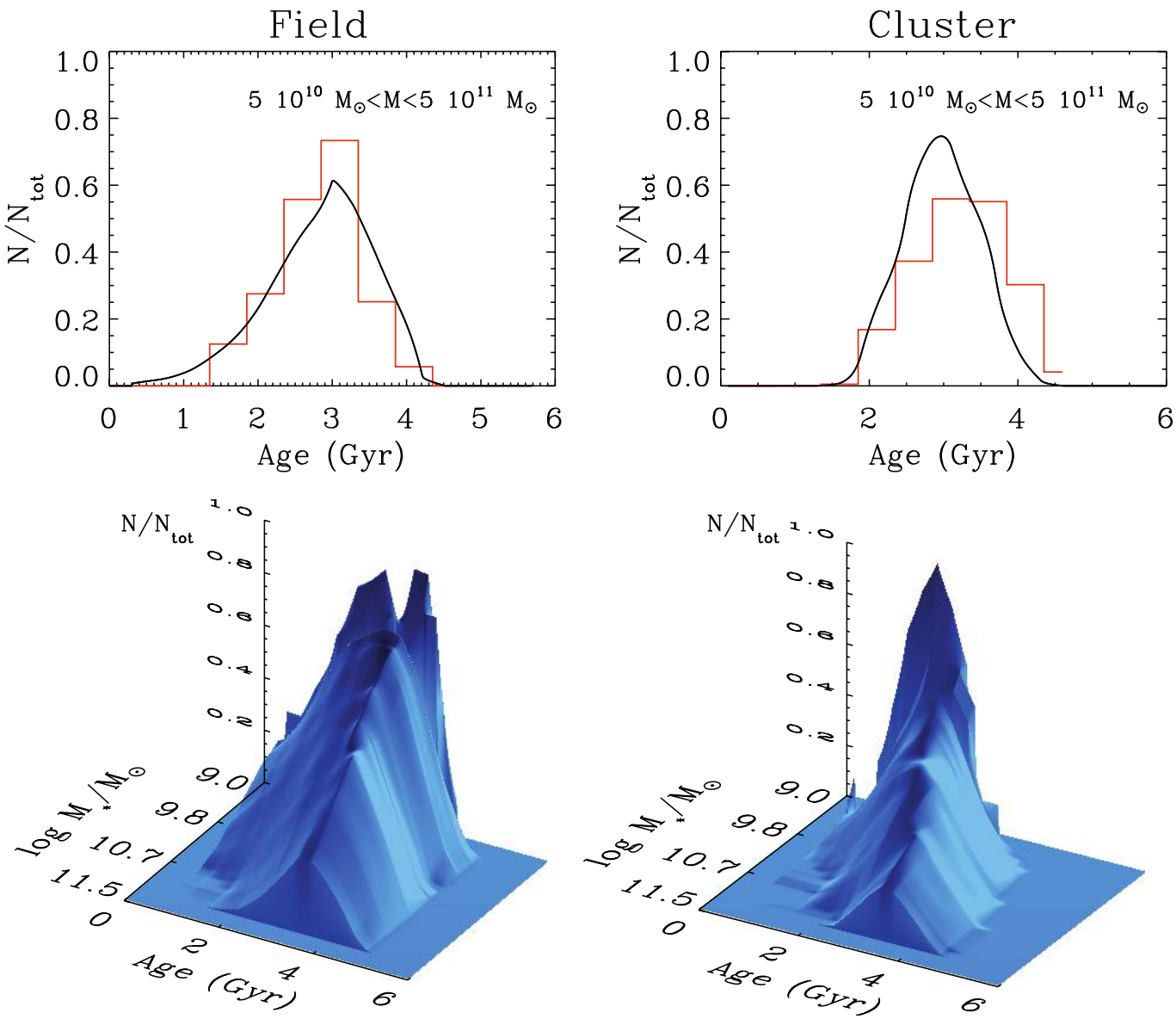

FIG. 7.—Distribution of stellar ages (see definition in the text) as a function of final stellar mass for galaxies in the field (*left*) and cluster (*right*) at $z = 1.2$. *Top panels*: The distribution of ages (*solid lines*) for galaxies in the mass range $5 \times 10^{10} \leq M_*/M_\odot \leq 5 \times 10^{11}$ at $z = 1.2$ in the field (*left*) and in clusters (*right*). The histograms represent the observed distributions of stellar ages derived, using eq. (1), from fitting with Bruzual-Charlot models the same spectrophotometric data as in Fig. 6 (Gobat et al. 2008). *Bottom panels*: The distribution of stellar ages (see definition in the text) as a function of final stellar mass for galaxies in the field (*left*) and clusters (*right*) at $z = 1.2$.

star formation in minor progenitors remains appreciable even at later cosmic times, and the scatter generated by the different merging histories effectively results into a final dispersion of galaxy color, ages, and stellar mass growth histories.

In other words, the model predicts that, for field galaxies, the formation of stellar populations finally included in a given galaxy is largely distributed among all its progenitors, while the majority of galaxies in clusters have been assembled earlier on into a single main progenitor, which hosts the bulk of the subsequent star formation.

Thus, although the overall (contributed by all progenitors) median star mass growth of field and cluster galaxies is similar (see Figs. 6 and 7), the scatter is considerably suppressed for the latter, since the variance introduced by the different merging histories is considerably reduced.

For completeness, we also show in the bottom panels of Figure 8 the cosmological evolution over the whole cosmic time of the predicted number of progenitors with stellar mass larger than 5×10^9 $M_\odot$. Note how, for field galaxies, this number remains large even at low redshift, indicating a delayed assembly of progenitors into a main object compared to cluster galaxies. Note also that a small number of massive progenitors is accreted also by cluster galaxies. Since the top right panel shows that their contribution to the buildup of the stellar mass is negligible when compared to the main progenitor, this implies that most of the minor clumps accreted by cluster galaxies are gas-poor, a condition due to the gas stripping caused by the surrounding cluster medium.

Thus, the different scatter of the RS between clusters and field results from the different balance between dry merging and star formation history of progenitors. That such a balance constitutes a key point in determining the properties of RS galaxies has been recently pointed out by Faber et al. (2007), who proposed that the building up of the RS results from a mixture of early star formation followed by quenching and dry merging, and noted that the prevalence of the latter would result in a reduced scatter of

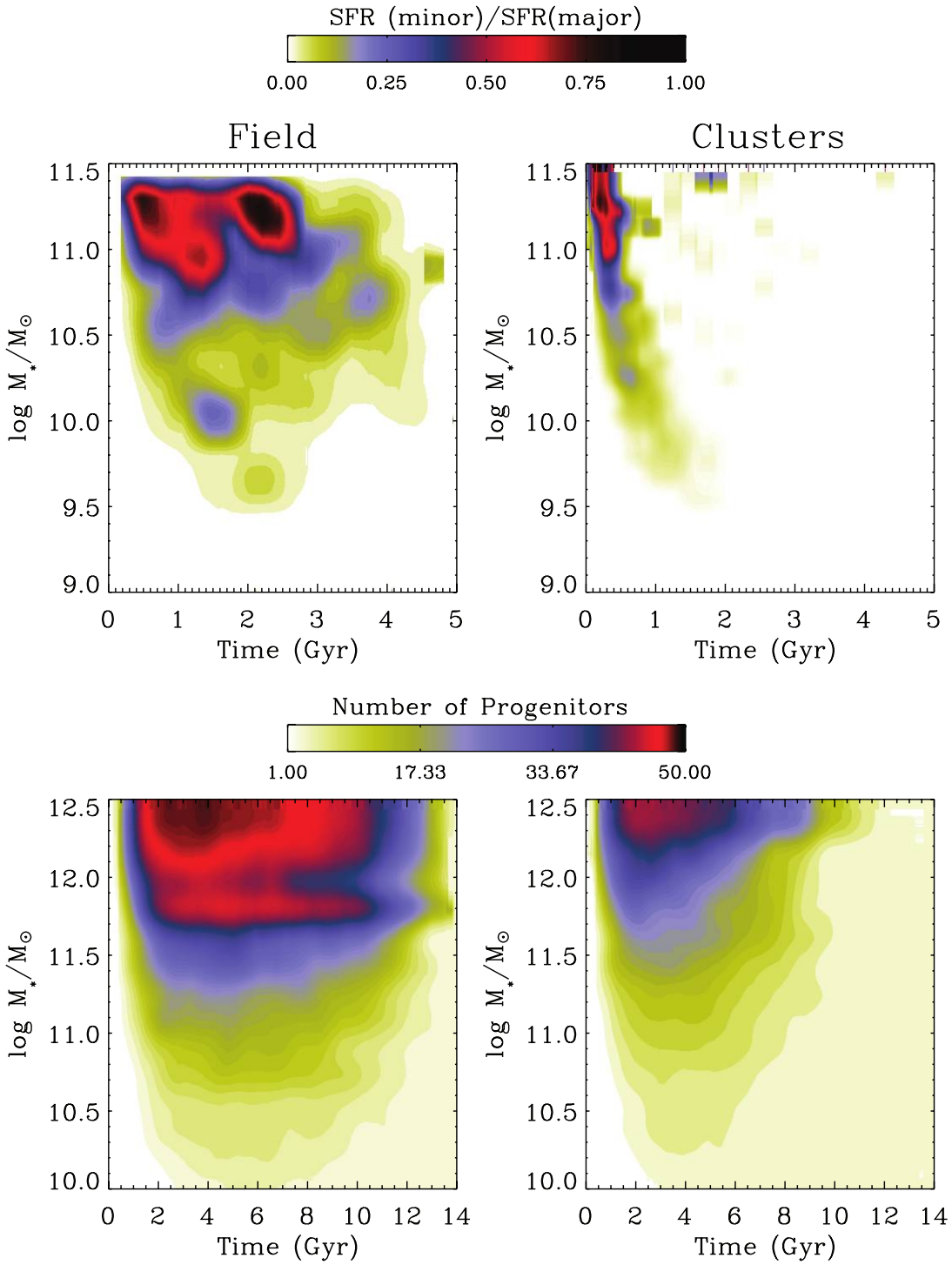

FIG. 8.—*Top panels*: The ratio between the star formation rate contributed by minor progenitors (see text for definition) and the main one (color code), plotted as a function of the cosmic time (*x*-axis) for different values of the final (at $z = 1.2$) stellar mass (*y*-axis). The left-hand column refers to field galaxies, and the right-hand column refers to cluster members. *Bottom panels*: The number of progenitors with stellar mass larger than 5×10^9 $M_\odot$ is represented by the colored contours as a function of cosmic time *t*, from $t = 0$ to the present for different values of the final (at $z = 0$) stellar mass (*y*-axis).

the RS. Here we argue that the balance between the two processes depends on the environment, with dry merging of progenitors with quenched star formation prevailing in biased environments (as results from the computation shown above). This leads in clusters to a relevant reduction not only of the RS scatter, but also of the scatter of the ages of the stellar populations of RS galaxies, a marker of the effect of dry merging already noted by Faber et al. (2007).

5. CONCLUSIONS

In this paper we have compared the results from a state-of-the-art semianalytic model of galaxy formation to spectrophotometric observations of the most distant galaxy clusters observed in the range $0.8 \lesssim z \lesssim 1.3$, to investigate the properties of the RS galaxies in high-redshift clusters and to compare them with those of the field in the same stellar mass range.

A long-standing prediction of cosmological galaxy formation models (see Kauffmann 1996; Diaferio et al. 2001) is that the *average* stellar populations of galaxies in clusters are older, since the star formation processes are accelerated in structures originated from overdense regions of the primordial density field. Recent observational progress (Baldry et al. 2004) has revealed in detail such an average reddening of galaxies for increasing environmental density, due to an increased population of the red branch of the bimodal color distribution. Thus, the redder *average* colors of the cluster galaxy populations we observe today are not caused by a global shift of the ages of the galaxy populations toward lower values, but instead by a different balance between the populations of the two branches of the color distribution.

In particular our results can be summarized as follows.

1. The speedup of the transition of galaxies from the blue cloud to the RS which takes place in dense environments is qualitatively reproduced by the hierarchical model for a wide range of galaxy masses (being faster for more massive galaxies) and cosmic times. In the case of distant galaxy clusters, the most extreme environments which provide the most challenging test for hierarchical models, such a fast transition in the model is able to reproduce a well-defined RS in clusters at $z \approx 1.3$, which is narrower than in the field, as observed. The fraction of galaxies which belong to the RS is larger in clusters than in the field from $z = 0$ to $z = 1.5$, and stays nearly constant in such an interval.

2. In agreement with observations, we find that at $z \approx 1.2$ the RS is not universal, i.e., it is subject to a cluster-to-cluster variance over the cluster population. The predicted color normalization is close to the observed average value and is distributed in a narrow range $\langle c \rangle \approx 0.9$–$1.1$, when different clusters are considered. Observations (e.g., Mei et al. 2006a, 2006b) suggest a cluster-to-cluster variation of $\sim$0.05 mag, a measurement which is limited by sample size and uncertainties in the *K*-correction and passive luminosity evolution in the redshift interval $0.8 \leq z \leq 1.3$.

3. The scatter of the model RS of cluster galaxies is found to be much tighter than that of the field by a factor ranging from 5 to 10. However, on average, they are still larger than the observed tight scatters ($\approx$0.05–0.08 mag), which are consistent only with the lower envelope of model distribution enclosing 75% of the clusters selected in the Monte Carlo simulation.

4. When *only* the RS galaxies are considered, the mass growth histories of field and cluster galaxies at $z \approx 1.2$ are similar. This is consistent with the mass growth derived from observations through SED and spectral fitting (Gobat et al. 2008) of massive early-type galaxies with adjustable star formation laws. Both observations and the model converge in indicating that at a cosmic time $t \approx 2.5$ Gyr more than 90% of the stellar mass finally assembled in the RS galaxies at $z = 1.2$ has already been formed in both field and clusters. The model also suggests that at cosmic times $t \approx 1$ Gyr the stellar mass fraction was about 50% in both field and clusters, whereas spectral synthesis modeling of the spectrophotometric data suggests a faster timescale in assembling stellar mass in clusters. Even though our model predicts the scatter of the growth histories to be larger in the field than in clusters, a slightly faster assembly timescale seems to be needed to account for the very tight observed RSs.

5. The corresponding predicted ages of the stellar populations in RS galaxies at $z \approx 1.2$ reflect the above behavior, with distributions peaking at values $\tau \approx 3.5$ Gyr in both field and clusters. These are consistent with the values derived from observations through SED + spectral fitting, although the latter indicate a slightly larger (by $\lesssim$0.5 Gyr) age for cluster RS galaxies, as compared with the model (Gobat et al. 2008; Rettura et al. 2008). The model prediction of a larger dispersion of ages for field RS galaxies compared to clusters is in good agreement with observations. Indeed, a negligible fraction of RS galaxies are predicted and observed to have ages shorter than 2 Gyr, while an appreciable—although minor—fraction ($\approx$0.2) of field RS galaxies have ages shorter than that.

6. The reduced scatter in color, ages, and stellar mass growth of cluster RS galaxies at $z \approx 1.2$ compared to field RS galaxies is originated from intrinsic properties of the merging histories of cluster galaxies. These are characterized by an earlier (compared to the field) assembly of galaxy progenitors into a main progenitor at times $t \lesssim 1.5$ Gyr. After such a time, the bulk of the stellar mass formation of cluster RS galaxies takes place in their main progenitor; thus, the scatter in mass growth histories, ages, and colors is considerably suppressed, since the variance introduced by the different merging histories is considerably reduced compared to the field, where the star formation is distributed among a larger number of progenitors.

The picture emerging from the above results is the following: For increasing cosmic time, the exhaustion of cold gas in galaxies and the subsequent decrease of the star formation activity drives the galaxies to flow from the "blue cloud" region of the color-magnitude space to the RS; the more massive the galaxies (and the earlier their gas conversion into stars), the earlier is the epoch of drift to the RS.

In dense environments, and in particular for high-redshift clusters, the drift of faint galaxies from the blue cloud to the RS is accelerated by various processes [namely, processes (i)–(iv) recalled in § 1] so that also fainter galaxies rapidly drift to the RS. As a result, the blue fraction in clusters is significantly smaller than in the field, and at high redshift a well-defined, narrow RS is already in place.

When only the galaxies that have drifted to the RS are considered, their *average star formation history* does not depend strongly on the environment and is not responsible for the reduced scatter of the RS in clusters compared to the field; the effect of the environment is to accelerate the drift to the RS (thus enhancing the relative population of the red branch compared to the blue branch in the color distribution) rather than changing the properties of the RS itself. This is supported by the detailed measurements of the color distribution of galaxies as a function of the environment in Baldry et al. (2004).

On the other hand, the *mass assembly history* of RS galaxies in clusters is considerably different from that occurring in the field, and has a significant impact on the scatter of the RS. Since cluster galaxies are formed from clumps that collapsed within high-density regions of the primordial density field, their assembly into a dominant progenitor is faster compared to the field, the formation of the bulk of the stellar mass of cluster RS galaxies takes place in their main progenitor, and the variance introduced to the star formation history by the different merging histories is considerably suppressed. The more biased the galaxy environment, the larger the above effect, so that for RS galaxies in high-redshift clusters the dispersion of mass growth histories, ages, and colors is appreciably reduced compared to the field.

Despite the overall good agreement between our models and observations on the color, luminosity, and mass distributions of galaxies in high- and low-density environments, our analysis has shown that even faster mass assembly or shorter star formation timescales are needed to reproduce the surprisingly tight RS in the massive clusters at $z \approx 1.2$ (see Fig. 5). This is extremely difficult to achieve in the model, since the dynamical history of DM halos does not constitute a tunable component for a given initial

power spectrum. Indeed, we have also verified that changing the normalization of the power spectrum, while affecting the abundance of clusters at a given redshift, is not effective in further narrowing down the scatter of the color-magnitude relation. Thus, we propose that the acceleration of mass assembly in cluster galaxies (making the bulk of the effect) must be complemented with a further acceleration of star formation in RS cluster galaxies. This is indicated also by the slight mismatch between model and observations in the stellar mass growth history (Fig. 6) and average ages (Fig. 7), when the RS cluster galaxies are considered. The modeling of such an additional enhancement of early star formation in the progenitors of cluster RS galaxies will probably require a finer treatment of the environmental dependence of the interaction-driven starbursts. An additional issue is the slope of the cluster RS obtained from the model. Current observations find no significant evolution with redshift of the RS slope, which remains close to $|\delta(U-B)/\delta B| \approx 0.04$ (Mei et al. 2008), whereas the model predicts a (nonevolving) flat slope. This can be due to both an overquenching of star formation at low masses, and also to a poor treatment of chemical evolution (e.g., the contribution of SN I is not properly accounted for in semianalytic models), which is known to affect the RS slope through metallicity effects (Kodama & Arimoto 1997).

Finally, we mention two additional consequences of our interpretation of the model results, both consistent with preliminary indications from observations. First, at redshift $z \gtrsim 1.5$ our model predicts the scatter of the cluster RS to extend to a wider range of values compared to the low-redshift interval $z \lesssim 1.5$ (see Fig. 4) and to easily reach values larger than 0.2 (see Fig. 5), consistent with preliminary results by Gobat et al. (2008). Second, the model predicts the speedup of star formation in dense environments to be larger for small-mass galaxies (with $M \lesssim 10^{10.5}\ M_{\odot}$; as inferred, e.g., by Fig. 3) compared to massive RS galaxies (which indeed are predicted to have similar mass assembly histories in the field and in clusters; see Fig. 6). This is also qualitatively consistent with preliminary results by Gobat et al. (2008), which indicate a lower average age of stellar populations in clusters only for galaxies with $M \lesssim 10^{11.2}\ M_{\odot}$. We will address in detail both points in a future paper.

We thank the referee for helpful comments, which contributed to improve the manuscript. We acknowledge grants from INAF and the ESO visitor programme. The National Radio Astronomy Observatory is a facility of the National Science Foundation operated under cooperative agreement by Associated Universities, Inc.

REFERENCES

Baldry, I. K., Balogh, M. L., Bower, R. G., Glazebrook, K., Nichol, R. C., Bamford, S. P., & Budavari, T. 2006, MNRAS, 373, 469
Baldry, I. K., Glazebrook, K., Brinkmann, J., Zeljko, I., Lupton, R. H., Nichol, R. C., & Szalay, A. S. 2004, ApJ, 600, 681
Balogh, M. L., Navarro, J. F., & Morris, S. L. 2000, ApJ, 540, 113
Bell, E. F., et al. 2004, ApJ, 608, 752
Bertin, E., & Arnouts, S. 1996, A&AS, 117, 393
Blakeslee, J., et al. 2003, ApJ, 596, L143
———. 2006, ApJ, 644, 30
Bond, J. R., Cole, S., Efstathiou, G., & Kaiser, N. 1991, ApJ, 379, 440
Bower, R. G., Benson, A. J., Malbon, R., Helly, J. C., Frenk, C. S., Baugh, C. M., Cole, S., & Lacey, C. G. 2006, MNRAS, 370, 645
Bower, R., Kodama, T., & Terlevich, A. 1998, MNRAS, 299, 1193
Bruzual, G., & Charlot, S. 2003, MNRAS, 344, 1000
Cavaliere, A., Colafrancesco, S., & Menci, N. 1992, ApJ, 392, 41
Cavaliere, A., & Vittorini, V. 2000, ApJ, 543, 599
Ciotti, L., & Ostriker, J. P. 1997, ApJ, 487, L105
Cooper, M. C., et al. 2006, MNRAS, 370, 198
Cowie, L. L., Songaila, A., Hu, E. M., & Cohen, J. G. 1996, AJ, 112, 839
Dekel, A., & Birnboim, Y. 2006, MNRAS, 368, 2
De Lucia, G., et al. 2007, MNRAS, 374, 809
Demarco, R., et al. 2007, ApJ, 663, 164
Diaferio, A., Kauffmann, G., Balogh, M. L., White, S. D. M., Schade, D., & Ellingson, E. 2001, MNRAS, 323, 999
Di Matteo, T., Springel, V., & Hernquist, L. 2005, Nature, 433, 604
Faber, S. M., et al. 2007, ApJ, 665, 265
Fabian, A. 1999, MNRAS, 308, L39
Gerke, B. F., et al. 2007, MNRAS, 376, 1425
Gobat, R., et al. 2008, A&A, in press (arXiv: 0806.4537v2)
Haehnelt, M. J., Natarajan, P., & Rees, M. J. 1998, MNRAS, 300, 817
Homeier, N. L., et al. 2006, ApJ, 647, 256
Hopkins, A. M. 2004, ApJ, 615, 209
Kauffmann, G. 1996, MNRAS, 281, 487
Kodama, T., & Arimoto, N. 1997, A&A, 320, 41
Lacey, C. G., & Cole, S. 1993, MNRAS, 262, 627
Lapi, A., Cavaliere, A., & Menci, N. 2005, ApJ, 619, 60
Larson, R. B., Tinsley, B. M., & Caldwell, C. N. 1980, ApJ, 237, 692
Mei, S., et al. 2006a, ApJ, 639, 81
———. 2006b, ApJ, 644, 759
———. 2008, ApJ, submitted
Menci, N., Cavaliere, A., Fontana, A., Giallongo, E., Poli, F., & Vittorini, V. 2003, ApJ, 587, L63
———. 2004a, ApJ, 604, 12
Menci, N., Fiore, F., Perola, G. C., & Cavaliere, A. 2004b, ApJ, 606, 58
Menci, N., Fontana, A., Giallongo, E., Grazian, A., & Salimbeni, S. 2006, ApJ, 647, 753
Menci, N., Fontana, A., Giallongo, E., & Salimbeni, S. 2005, ApJ, 632, 49
Neistein, E., van den Bosch, F. C., & Dekel, A. 2006, MNRAS, 372, 933
Rettura, A., et al. 2006, A&A, 458, 717
———. 2008, ApJ, in press (arXiv: 0806.4604v1)
Romeo, A. D., Napolitano, N. R., Covone, G., Sommer-Larsen, J., Antonucci-Delogu, V., & Capaccioli, M. 2008, MNRAS, 389, 13
Silk, J., & Rees, M. J. 1998, A&A, 331, L1
Spitzer, L., Jr., & Baade, W. 1951, ApJ, 113, 413
Strateva, I., et al. 2001, AJ, 122, 1861
Strazzullo, V., et al. 2006, A&A, 450, 909
Vanzella, E., et al. 2008, A&A, 478, 83
Weinmann, S. M., van der Bosch, F. C., Yang, X., & Mo, H. J. 2006, MNRAS, 366, 2